

Anti-tumor effects of 2-oxoglutarate through inhibition of angiogenesis in a murine tumor model

Ken Matsumoto^{1*}, Naoshi Obara¹, Masatsugu Ema³, Masaki Horie², Ayano Naka²,
Satoru Takahashi³ and Shigehiko Imagawa^{2*}

1. Division of Hematology, Institute of Clinical Medicine, University of Tsukuba, Tsukuba, Ibaraki 305-8575, Japan
2. Doctoral Program of Sports Medicine, University of Tsukuba, Tsukuba, Ibaraki, Japan
3. Department of Anatomy and Embryology, Institute of Basic Medical Sciences, Graduate School of Comprehensive Human Sciences, University of Tsukuba, Ibaraki, Japan

*Please send correspondence to:

Ken Matsumoto, Division of Hematology, Institute of Clinical Medicine,
University of Tsukuba, Tsukuba, Ibaraki 305-8577, Japan

TEL & FAX: 81-29-853-8353, E-mail: c0630210@md.tsukuba.ac.jp

Or

Shigehiko Imagawa, Doctoral Program of Sports Medicine, University of Tsukuba,
Tsukuba, Ibaraki, Japan

Scientific heading: Anti-tumor effect of 2-oxoglutarate *in vivo*

Keywords: 2-oxoglutarate, HIF-1, VEGF, Angiogenesis

Total number of text figures:

This work was supported by grants-in-aid for scientific research from the Ministry of Education, Science and Culture of Japan.

Summary

Hypoxia-inducible factor 1 (HIF-1) plays essential roles in tumor angiogenesis and growth by regulating the transcription of several key genes in response to hypoxic stress and growth factors. HIF-1 is a heterodimeric transcriptional activator consisting of inducible α and constitutive β subunits. In oxygenated cells, proteins containing the prolyl hydroxylase domain (PHD) directly sense intracellular oxygen concentrations. PHDs tag HIF-1 α subunits for polyubiquitination and proteasomal degradation by prolyl hydroxylation using 2-oxoglutarate (2-OX) and dioxygen. Our recent studies showed that 2-OX reduces HIF-1 α , erythropoietin and vascular endothelial growth factor (VEGF) expression in the hepatoma cell line Hep3B when under hypoxic conditions *in vitro*. Here, we report that similar results were obtained in Lewis lung cancer (LLC) cells in *in vitro* studies. Furthermore, 2-OX showed potent anti-tumor effects in a mouse dorsal air sac (DAS) assay and a murine tumor xenograft model. In the DAS assay, 2-OX reduced the numbers of newly formed vessels induced by LLC cells. In a murine tumor xenograft model, intraperitoneal injection of 2-OX significantly inhibited tumor growth and angiogenesis in tumor tissues. Moreover, 5-fluorouracil combined with 2-OX significantly inhibited tumor growth in this model, which was accompanied by reduction of *Vegf* gene expression in tumor tissues. These results suggest that 2-OX is a promising anti-angiogenic therapeutic agent.

Introduction

The growth of solid tumors is frequently accompanied by neovascularization. This requirement for angiogenesis implied that targeting tumor vascular endothelial cells might represent a novel therapeutic strategy⁽¹⁾. Proof of principle was established through clinical applications demonstrating efficacy of the anti-vascular endothelial growth factor (VEGF) antibody, bevacizumab⁽²⁾.

VEGF is a potent angiogenic factor and endothelial cell-specific mitogen^(3, 4, 5) that is regulated by hypoxia *in vitro*⁽⁶⁾ and *in vivo*^(7, 8, 9, 10). This hypoxic induction of VEGF is due to an increase in the steady state level of *Vegf* mRNA⁽¹¹⁾. Similar to the erythropoietin (*Epo*) gene⁽⁶⁾, the *Vegf* gene is induced by metal ions and hypoxia⁽¹⁰⁾. The implication of these studies is that there may be fundamental similarities in the oxygen-sensing pathway leading to the activation of these two genes. Hypoxic induction of the *Epo* gene appears to be regulated by both transcriptional and post-transcriptional mechanisms^(12, 13, 14). Hypoxia-inducible factor 1 (HIF-1) was identified as a protein that specifically binds to an enhancer element 3' to the *Epo* gene in a hypoxia-regulated fashion^(15, 16).

HIF-1 is a key regulator of responses to hypoxia, occupying a central position in oxygen homeostasis in a wide range of organisms⁽¹⁷⁾. Among its transcriptional targets are genes with critical roles in angiogenesis, erythropoiesis, energy metabolism, vasomotor function, and apoptotic/proliferative responses. HIF-1 is also essential for normal development⁽¹⁸⁾ and plays key roles in pathophysiological responses to ischemia/hypoxia as well as in tumor growth and angiogenesis⁽¹⁷⁾.

HIF-1 is a heterodimeric transcription factor composed of a HIF-1 α subunit and a HIF-1 β subunit⁽¹⁹⁾. HIF-1 α is continuously synthesized and degraded under normoxic conditions.

Under hypoxic conditions, HIF-1 α degradation is inhibited, allowing the protein to accumulate and dimerize with HIF-1 β . This heterodimer binds to cis-acting hypoxia-response elements in target genes and recruits coactivator proteins, all of which leads to increased transcription. In oxygenated cells, intracellular oxygen concentrations are directly sensed by HIF-1 α hydroxylation enzymes, prolyl hydroxylases (PHDs). PHDs tag HIF-1 α subunits for polyubiquitination and proteasomal degradation by prolyl hydroxylation using 2-oxoglutarate (2-OX) and dioxygen^(20, 21). Our recent studies have shown that 2-OX reduces HIF-1 α , erythropoietin, and VEGF expression under hypoxic conditions in the hepatoma cell line Hep3B⁽²²⁾. To address the clinical usefulness of 2-OX, we investigated its anti-tumor effect using a mouse dorsal air sac (DAS) assay and a murine tumor xenograft model. We found that 2-OX exerts potent anti-tumor effects by inhibiting angiogenesis, and we discuss the possibility of 2-OX as a novel anti-angiogenesis drug.

Material and Methods

Cell culture. The Lewis lung carcinoma (LLC) and B16F10 melanoma cell lines were obtained from the American Type Tissue Culture Collection (Rockville, MD, USA). Cells were incubated under both 21% (normoxia) and 1% (hypoxia) oxygen. The exposure times were as described below.

Cell proliferation assay. Cell survival was determined by a nonradioactive cell proliferation assay (Promega, WI, USA). LLC cells (1.5×10^4 cells) in a 96-well plate (Nunc A/S, Roskilde, Denmark) were incubated for 24 h. Then the medium was changed to new medium containing various concentrations of 2-OX (Fluka, Buchs, Switzerland) and incubated under normoxic

(21% O₂) or hypoxic (1% O₂) conditions for 20h. After incubation, the tetrazolium component of the Dye Solution was added. After incubation for 4 h, the Solubilization/Stop Solution was added to the cultures to solubilize the formazan product, and the absorbance reading at 570 nm was recorded by a 96-well plate reader (Bio-Rad, CA, USA).

Semi-quantitative RT-PCR. We used the following primers for RT-PCR: HIF-1 α -sense, 5'-GAGTTCTGAACGTCGAAAAG-3'; HIF-1 α -antisense, 5'-CTCACACGTAATAACTGATGG-3'; HIF-2 α -sense, 5'-GGACGCTCTGCCTATGAGTT-3'; HIF-2 α -antisense, 5'-GGCTCCTCCTTCAGTTTGG-3'; β -actin-sense, 5'-GTGCTATGTTGCCCTGGATT-3'; β -actin antisense, 5'-TGCTAGGGCTGTGATCTCCT-3'. We extracted RNA using the RNeasy kit (Qiagen) . Total RNA (1 μ g) was primed with 0.5 μ g of oligo dT and reverse transcribed by Omniscript reverse transcriptase using a primeScript RT-PCR kit (Takara). PCR proceeded using the cDNA as a template and TakaRa EX TaqTM HS (Takara) . The number of PCR cycles determined from the plot was thirty for both HIF-1 α and HIF-2 α and 25 for β -actin.

Western blot analysis. Nuclear extracts (15 μ g) prepared from LLC cells were electrophoresed on a 7.5% sodium dodecyl sulfate (SDS)-polyacrylamide gel and transferred onto a polyvinylidene difluoride membrane (Millipore, Billerica, MA, USA). Blocking was performed at room temperature for 1 h in phosphate-buffered saline (PBS) containing 5% nonfat milk. The membranes were incubated with anti-HIF-1 α antibody (Lab vision, Fremont, CA, USA) in PBS containing 5% nonfat milk. After washing with PBS containing 0.1% Tween 20, the membrane was incubated with horseradish peroxidase-conjugated goat anti-mouse IgG (Zymed, San Francisco, CA, USA) in PBS containing 5% nonfat milk. Subsequently, proteins were detected by

enhanced chemiluminescence (Millipore). Goat anti-lamin B antibody (Santa Cruz Biotechnology, Santa Cruz, CA, USA) was used to monitor protein loading and transfer efficiency.

Quantitative RT-PCR. We extracted RNA using the RNeasy kit (Qiagen). Total RNA (1 μ g) was primed with 0.5 μ g of oligo dT and reverse transcribed by Omniscript reverse transcriptase using a PrimeScript RT-PCR kit (Takara). The reaction was performed at 42°C for 30 min. The mRNA expression levels were analyzed by real-time quantitative PCR with TaqMan probe using an applied Biosystems 7500 Real-time PCR system (Perkin-Elmer Applied Biosystems, Foster, CA, USA) as previously described. The expression of *Actin* mRNA was used as an internal control. The PCR mixture (25 μ L total volume) consisted of FAM-labeled primer probes (Roche Diagnostics GmbH, Mannheim, Germany) and FastStart Universal Probe Master [ROX] (Roche Diagnostics GmbH). Each PCR amplification was performed in triplicate, using the following profile: one cycle of 95°C for 10min, 40 cycles of 94°C for 15 s, and 60°C for 1 min. The quantitative values of target mRNA were normalized to that of actin mRNA expression.

ELISA. To determine the levels of VEGF protein from the LLC cells, commercial enzyme-linked immunosorbent assays (ELISA: mouse VEGF; R&D systems, Minneapolis, MN) were used. ELISA was performed following the recommendations of the manufacturer. The detection limits is 3 pg/mL for VEGF.

Mice. Seven-week-old male C57BL/6J mice were purchased from Clea-Japan (Tokyo, Japan). They were housed in autocleaning metal cages in an air-conditioned room and were offered a standard diet (CM; Oriental Yeast, Tokyo, Japan) and tap water *ad libitum*. This study was approved in accordance with the Regulations for Animal Experimentation at the University of Tsukuba and the Law on Human Treatment and Management of Animals (Law No. 105 of

Japan).

Mouse Dorsal Air Sac (DAS) Assay. Tumor-induced blood vessel formation was assessed as described previously ⁽²³⁾. In brief, Millipore chambers (Millipore) were filled with either PBS alone or a suspension of 1.5×10^7 LLC cells in PBS with or without 2-OX and sealed with membrane filters (0.45 μm pores). Chambers were implanted subcutaneously in dorsal air sacs created surgically by injection of an appropriate volume of air in seven-week-old male C57BL/6J mice. Four days later, mice were given an overdose of diethyl ether. The skin was carefully removed and angiogenesis that had been induced around the chamber was examined under a stereomicroscope and photographed. Quantitative analyses were performed with angiogenesis-measuring software (version 2.0; Kurabo, Osaka, Japan). Each experimental group included four mice, and each experiment was repeated at least twice. No obvious adverse effects appeared after treatment of animals with 2-OX. All surgical procedures were performed under pentobarbital anesthesia (Dainabot, Osaka, Japan).

Effect of 2-OX on growth of LLC cells *in vivo*. Cells in PBS were implanted into the right flank region of seven-week-old C57BL/6J mice. Daily intraperitoneal injections of 2-OX were started the day after implantation. From six to twelve days after implantation, we measured tumors with calipers and calculated volumes as $(\text{length} \times \text{width}^2) \times 0.5$. LLC tumors were removed from mice twelve days after implantation for quantitative RT-PCR and immunohistochemical studies.

Effect of 2-OX and/or 5-fluorouracil (5-FU) on growth of LLC cells *in vivo*. Cells in PBS were implanted into the right flank region of seven-week-old C57BL/6J mice. Mice were randomly assigned to four groups: (1) PBS alone, (2) 2-OX alone, (3) 5-FU alone, and (4) 5-FU +2-OX. For all groups, 5-FU was injected intraperitoneally on day 7 and 2-OX was injected

intraperitoneally daily from day 7-15. From six to fifteen days after implantation, we measured tumors with calipers and calculated volumes as $(\text{length} \times \text{width}^2) \times 0.5$. LLC tumors were removed from mice fifteen days after implantation for quantitative RT-PCR.

Immunohistochemistry and vessel density determination. Tumors were fixed overnight in 4% paraformaldehyde in PBS. Half of the tumor was frozen, and cryosectioning was carried out at a thickness of $5 \mu\text{m}$ for immunohistochemical staining. Briefly, all tissue sections were permeabilized with 0.1% Triton X-100 (Sigma, St Louis, MO, USA), blocked with goat normal serum for 30min for nonspecific binding, and then incubated with a rat monoclonal antibody against mouse CD31 (Pharmlingen BD, Stockholm, Sweden) overnight at 4°C . Primary antibodies were detected with secondary chicken anti-rat IgG conjugated to Alexa 488 (Molecular Probes Inc., Eugene, OR, USA) for immunofluorescence detection and nuclei were counterstained with 4,6-diamidino-2-phenylindole (DAPI). Quantitative analyses were performed with angiogenesis-measuring software (Kurabo).

Statistical analysis. Student's *t* tests were used to assess the level of significance between the treatment groups.

Results

2-OX reduces HIF-1 α protein level in cultured LLC cells. Our previous studies showed that 2-OX reduces HIF-1 α , Epo and VEGF expression in a hepatoma cell line Hep3B when grown under hypoxic conditions. This implies that 2-OX may be able to reduce tumor growth by inhibition of HIF-1 activity in the tumor because VEGF induction by hypoxia is responsible for tumor growth and angiogenesis. In order to evaluate the effect of 2-OX on LLC tumor growth in an animal model, we first investigated the cytotoxic effect of 2-OX on LLC tumor cells. Cell cytotoxicity was determined by a cell proliferation assay following the addition of 2-OX to LLC cells. There was no cell cytotoxicity up to 15 mM 2-OX (Fig.1A). LLC cells express HIF-1 α mRNA, but not HIF-2 α mRNA (Fig. 1B). To elucidate the effect of 2-OX on the production of HIF-1 α protein in LLC cells, western blot analysis was performed. Compared with normoxia, hypoxia markedly induced the expression level of HIF-1 α protein (Fig. 1C, upper panel, lane 2). However, the addition of 7.5 and 15 mM 2-OX dose-dependently reduced HIF-1 α protein production (Fig. 1C, upper panel), although the addition of 2-OX did not affect lamin B, which was used as a control (Fig.2B, lower panel). These results suggest that 2-OX reduces the HIF-1 α protein level.

2-OX reduces *Vegf* mRNA and protein levels in cultured LLC cells. *Vegf* mRNA expression induced by 1.5 hr hypoxic treatment in LLC cells was 1.65 ± 0.12 -fold times that of the normoxic control (Fig.2A). To elucidate the dose-dependent effects of 2-OX on *Vegf* mRNA expression in LLC cells, different concentrations of 2-OX were added to the cultures. Addition of 7.5 and 15 mM 2-OX decreased *Vegf* mRNA expression to 1.47 ± 0.12 and 1.29 ± 0.14 times that of the normoxic control, respectively (Fig.2A). *Vegf* mRNA expression in LLC cells induced by 3 hr hypoxia treatment was 3.70 ± 0.55 -fold times that of the normoxic control

(Fig.2A) . Addition of 7.5 and 15 mM 2-OX reduced the *Vegf* mRNA level to 3.32 ± 0.26 and 1.97 ± 0.27 times that of the normoxic control, respectively (Fig.2A) . These results indicate that 2-OX inhibits *Vegf* mRNA expression in LLC cells in a dose-dependent manner.

To evaluate the VEGF protein levels after 2-OX treatment, an ELISA assay was performed. Hypoxia-induced VEGF protein production from LLC cells was 289.3 ± 25.6 pg/mg protein (Fig.2B). To elucidate the dose-dependent effects of 2-OX on the production of VEGF by LLC cells, different concentrations of 2-OX were added to the cultures. Addition of 7.5 or 15 mM 2-OX inhibited VEGF protein production to 253.5 ± 17.8 and 178.6 ± 23.7 pg/mg protein, respectively (Fig.2B). These results indicate that 2-OX inhibits VEGF protein production by LLC cells in a dose-dependent manner. Thus, consistent with the reduction of VEGF mRNA, VEGF protein is reduced by 2-OX treatment in a dose-dependent manner in LLC cells.

2-OX inhibits blood vessel formation *in vivo*. To assess the effect of 2-OX on tumor angiogenesis *in vivo*, we performed DAS assays using LLC cells. When mice were implanted with a chamber that carried LLC cells, blood vessels characterized by strikingly disorganized and tortuous vessels were induced towards the chamber from pre-existing blood vessels beneath the epidermis (Fig.3A). Such tumor-induced blood vessel formation was, however, reduced by the administration of 2-OX (Fig.3A). Quantitative analysis of the values of blood vessel area by LLC cells using angiogenesis-measuring software were as follows: LLC only, $100 \pm 20.8\%$; LLC+7.5mM 2-OX, $64.0 \pm 9.4\%$; and LLC+15mM 2-OX, $45.6 \pm 4.4\%$ (Fig.3A) . In contrast, 2-OX had little influence on the pre-existing blood vessels under the chamber (Fig.3B) . In this model, 2-OX showed significant dose-dependent anti-angiogenic effects, reducing the number of newly formed vessels induced by LLC cells. This result indicates that 2-OX clearly inhibited the angiogenesis induced by LLC cells in a dose-dependent manner.

2-OX inhibits tumor growth and angiogenesis *in vivo*. To assess the effect of 2-OX on tumor growth, we injected 2-OX into mice with solid tumors. Tumor volumes and weights twelve days after implantation were as follows: PBS alone, $330.8 \pm 108.1 \text{ mm}^3$ and $192.6 \pm 66.4 \text{ mg}$; 50mg/kg 2-OX, $128.8 \pm 16.4 \text{ mm}^3$ and $111.0 \pm 64.5 \text{ mg}$; and 100mg/kg 2-OX, $78.7 \pm 43.7 \text{ mm}^3$ and $88.8 \pm 57.5 \text{ mg}$ (Fig.4A, B, C) . These data indicate that 2-OX reduces tumor size. We observed significant differences in microvessel density (PBS alone, $100 \pm 16.5 \%$; and 100mg/kg 2-OX, $46.0 \pm 13.5 \%$) by immunostaining for the endothelial cell marker CD31 (Fig.5A, B) . 2-OX treatment (100mg/kg) tended to decrease the expression level of the *Vegf* gene in tumor tissues compared with the control by quantitative RT-PCR (Fig.5C) . In this xenograft model, intraperitoneal injection of 2-OX significantly inhibited tumor growth and angiogenesis in tumor tissues. We observed that topical 2-OX treatment reduced tumor growth in C57BL/6J mice bearing LLC tumors (data not shown) .

2-OX in combination with 5-FU chemotherapy clearly inhibited tumor growth and tissue *Vegf* expression *in vivo*. Anti-VEGF antibody bevacizumab has been used clinically to reduce tumor growth in combination with chemotherapeutic reagents such as 5-FU⁽²⁵⁾ . To assess the effect of 2-OX in combination with 5-FU on tumor growth, we injected 2-OX and 5-FU intraperitoneally in mice with solid tumors. Tumor volumes and weights fifteen days after implantation were as follows: PBS alone, $531.2 \pm 144.9 \text{ mm}^3$ and $306.3 \pm 186.6 \text{ mg}$; 2-OX alone, $324.0 \pm 156.5 \text{ mm}^3$ and $308.7 \pm 299.0 \text{ mg}$; 5-FU alone, $287.1 \pm 155.2 \text{ mm}^3$ and $204.7 \pm 108.9 \text{ mg}$; and 5-FU + 2-OX, $98.7 \pm 64.9 \text{ mm}^3$ and $130.3 \pm 113.5 \text{ mg}$ (Fig.6A, B, C) . 5-FU combined with 2-OX significantly inhibited tumor growth in this model, which was accompanied by a 53% reduction of *Vegf* gene expression in tumor tissues removed from mice fifteen days after implantation as determined by quantitative RT-PCR analysis (Fig.6D) .

Discussion

Since the concentration of 2-OX and dioxygen is essential for hydroxylation and degradation of HIF-1 α protein, consistent with this report, Jaakkola et al. examined a series of 2-OX analogs that act as competitive inhibitors of PHDs⁽²⁶⁾ for their ability to inhibit HIF-PHD⁽²¹⁾. We also reported that 2-OX treatment of Hep3B cells induced HIF-1 α degradation *in vitro* and reduced the production of VEGF protein⁽²²⁾. Treatment with 2-OX also restored PHD2 to control levels and abolished the nuclear accumulation of HIF-1 α ⁽²⁷⁾. Based on cell culture studies, cell-permeating 2-OX derivatives have been proposed as a new therapy to restore normal PHD activity and HIF-1 α levels to those of succinate dehydrogenase-suppressed cells⁽²⁸⁾. These *in vitro* studies indicate that 2-OX induces HIF-1 α degradation and suppresses gene expression downstream of HIF-1. However, it was not clear whether 2-OX could be useful for suppression of tumor angiogenesis and its growth in animals. Our current study clearly shows that 2-OX reduced the HIF-1 α protein level in LLC cells and reduced LLC cell-induced tumor angiogenesis in an animal model. 2-OX also reduced tumor growth in a dose-dependent manner.

It is widely recognized that targeting tumor endothelial cells is useful for tumor therapy. Bevacizumab, a neutralizing antibody against VEGF, has been used for various tumor therapies in combination with chemoreagents⁽²⁵⁾. In the present study, we evaluated the effect of 2-OX on tumor angiogenesis in a DAS model. Addition of 2-OX clearly reduced LLC tumor growth in a dose-dependent manner. Furthermore, combining 2-OX and 5-FU revealed more drastic anti-tumor activity compared with single injections. It is of note that the *Vegf* mRNA level was reduced in the 2-OX and 5-FU-treated tumor, suggesting that downregulation of *Vegf* mRNA may account, in part, for the reduced tumor growth. Taken together, 2-OX could be an effective

chemotherapeutic reagent in combination with 5-FU.

Among the three members of the HIF-PHD genes, PHD2 may play a major role in HIF1 α hydroxylation during hypoxia. However, it is not clear that HIF-1 α destabilization by 2-OX is mediated by PHD2. Further studies will be required for clarification of the molecular mechanism of 2-OX action during the inhibition of tumor angiogenesis and growth.

Small chemical molecules that activate or inhibit HIF-PHD are reported. Choi et al. found a potent activator of PHD2 called KRH102053 ⁽²⁹⁾. The effects of KRH102053 on controlling HIF were studied in cell lines. Under their experimental conditions, KRH102053 decreased the protein level of HIF-1 α and the mRNA levels of HIF-regulated downstream target genes, such as VEGF, aldolase A, enolase 1 and monocarboxylate transporter 4, in cell models. Inhibition of HIF-PHD mimics hypoxia, stabilizes HIF, and stimulates *Epo* gene expression, even under normoxic conditions. FibroGen has recently developed a new HIF-PHD inhibitor called FG-2216 ⁽³⁰⁾. It completed a phase I study of FG-2216 using 54 healthy subjects in the UK and is conducting a phase II study of FG-2216 involving 42 patients with chronic kidney diseases or chemically induced anemia in Germany and Poland ⁽³⁰⁾. Doses of 6 mg/kg of FG-2216 and higher cause a dose-dependent elevation of serum EPO, which increased hemoglobin concentrations by 1.1 g/dL above the baseline level on day 42 of the study ⁽³⁰⁾. However, as expected, based on the effects of HIF-PHD, there is concern that FG-2216 might increase expression of VEGF. The same is equally true of whole body 2-OX administration.

2-OX is a metabolite in the TCA cycle and exists in cells at relatively high concentrations. Our study clearly showed that various concentrations had no effect on the viability of cultured cells but were sufficient to reduce tumor size. Further, 2-OX had no effect on pre-existing endothelial cells and had no effect on blood cell count in peripheral blood samples that were

obtained from the retro-orbital plexus of mice (data not shown) . Taken together, 2-OX is a promising new therapeutic reagent with no apparent side effects for inhibiting tumor angiogenesis and tumor size.

Hypoxia has been shown to be a very important stimulus for new vessel formation as seen in coronary artery disease ⁽³¹⁾ and diabetic neovascularization ⁽³²⁾. HIF-1 is a key transcription factor regulating oxygen homeostasis. Arjamaa et al. showed that all oxygen-dependent diseases of the retina are regulated by HIF ⁽³³⁾ . Thus, it will be very interesting to investigate in future if 2-OX inhibits other HIF-dependent diseases in animal models.

Figure Legends

Fig. 1

Fig. 1. Effect of 2-OX on HIF-1 α and HIF-2 α mRNA and protein expression in cultured LLC. (A) Effect of 2-OX on LLC cell proliferation. LLC cells were incubated with the indicated concentrations of 2-OX under normoxic or hypoxic conditions. Cell viability was measured by a nonradioactive cell proliferation assay. The number of living cells incubated without 2-OX was expressed as 100%. Error bars represent 1 SD (n = 9). Normoxia, 21 % O₂; Hypoxia, 1 % O₂. # indicates significance compared with normoxic control, P < 0.001. ## indicates significance compared with normoxic control, P < 0.01. * indicates significance compared with hypoxic control, P < 0.001. (B) Effect of 2-OX on HIF-1 α and HIF-2 α mRNA expression. LLC and B16F10 cells were incubated with and without 2-OX under normoxic or hypoxic conditions. HIF-1 α and HIF-2 α mRNAs were detected by

semi-quantitative RT-PCR. Normoxia, 21 % O₂; Hypoxia, 1 % O₂. (C) Effect of 2-OX on enhanced expression of HIF-1 α protein production in cultured LLC. LLC cells were treated with the indicated concentrations of 2-OX under normoxic or hypoxic conditions for 1.5 h. The cells were then lysed, and protein was detected with anti-HIF-1 α and lamin B antibodies by western blotting. The autoradiograph is representative of four different experiments using different cell extracts. Numbers below the bands are means \pm 1 SD as determined by densitometric analysis of the ratio of the bands (HIF-1 α / lamin B) expressed relative to lane 2. Triangle indicates HIF-1 α . Normoxia, 21 % O₂; Hypoxia, 1 % O₂. * indicates significance compared with control, P < 0.05. **indicates significance compared with control, P < 0.001.

Fig. 2. Effect of 2-OX on *Vegf* mRNA and protein expression in cultured LLC. (A) Effect of 2-OX on *Vegf* mRNA expression. LLC cells were incubated with and without 2-OX under normoxic or hypoxic conditions. *Vegf* mRNA expression was measured by quantitative RT-PCR. Three separate experiments (hypoxia exposure time, 1.5h) and six separate experiments (hypoxia exposure time, 1.5 h) were performed. Error bars represent 1 SD. Normoxia, 21 % O₂; Hypoxia, 1 % O₂. #indicates significance compared with hypoxic control (hypoxia exposure time, 1.5h) , P < 0.05. ## indicates significance compared with hypoxic control (hypoxia exposure time, 3h) , P < 0.001. * indicates significance compared with hypoxic control (hypoxia exposure time, 3h) , P < 0.001. (B) Effect of 2-OX on VEGF protein production from LLC cells. LLC cells were incubated with and without 2-OX under normoxic or hypoxic conditions. VEGF protein was measured by ELISA. Five separate experiments were performed. Error bars represent 1 SD. Normoxia, 21 % O₂; Hypoxia, 1 % O₂. * indicates significance compared with hypoxic control, P < 0.001. ** indicates significance compared with hypoxic control, P < 0.05.

Fig. 3. Effect of 2-OX on *in vivo* blood vessel formation by DAS assay. Chambers filled with either PBS alone or PBS plus LLC cells with or without 2-OX were implanted into seven-week-old mice. The dorsal skin was peeled off, and blood vessel formation was examined under a microscope and photographed. Scale bar, 3 mm. Area of tumor-induced blood vessels were analyzed with angiogenesis-measuring software. A representative result from three independent experiments with similar results is shown. Four separate experiments were performed. Error bars represent 1 SD. * indicates significance compared with LLC only, $P < 0.01$. ** indicates significance compared with LLC only, $P < 0.05$.

Fig.4. Effect of 2-OX on growth of LLC cells *in vivo*. Cells in PBS were implanted into the right flank region of seven-week-old C57BL/6J mice. Daily intraperitoneal injections of 2-OX were started the day after implantation. From six to twelve days after implantation, we measured tumors with calipers and calculated volumes as $(\text{length} \times \text{width}^2) \times 0.5$. (A) Tumor volume. (B) Gross appearance of xenografts and excised tumors at day 12. Scale bar, 5mm. (C) Tumor weight at day 12. A representative result from three independent experiments with similar results is shown. Five separate experiments were performed. Error bars represent 1 SD. *indicates significance compared with control, $P < 0.001$. ** indicates significance compared with control, $P < 0.01$. *** indicates significance compared with control, $P < 0.025$. **** indicates significance compared with control, $P < 0.05$.

Fig.5 Effect of 2-OX on microvessel density in LLC tumors. Cells in PBS were implanted into the right flank region of seven-week-old C57BL/6J mice. Daily intraperitoneal injections of

2-OX were started the day after implantation. LLC tumors were removed from mice twelve days after the implantation for immunohistochemical studies. (A) Immunohistochemical studies for CD31 and blood vessel formation was examined under a microscope and photographed. Scale bar, 150 μ m. (B) Area of microvessel density was analyzed with angiogenesis-measuring software. A representative result from three independent experiments with similar results is shown. Four separate experiments were performed. Error bars represent 1 SD. *indicates significance compared with control, $P < 0.005$. (C) Effect of 2-OX on *Vegf* mRNA expression in LLC tumor. Cells in PBS were implanted into the right flank region of seven-week-old C57BL/6J mice. Daily intraperitoneal injections of 2-OX were started the day after implantation. LLC tumors were removed from mice twelve days after the implantation for quantitative RT-PCR. Nine separate experiments were performed. Error bars represent 1 SD. *Vegf* mRNA levels in LLC tumors were quantified by quantitative RT-PCR and normalized to the level of *Actin* mRNA.

Fig.6. Effect of 2-OX and/or 5-FU on growth of LLC cells *in vivo*. Cells in PBS were implanted into the right flank region of seven-week-old C57BL/6J mice. Intraperitoneal injections of the indicated cocktails occurred daily beginning on day 7 after implantation. From six to fifteen days after implantation, we measured tumors with calipers and calculated volumes as $(\text{length} \times \text{width}^2) \times 0.5$. (A) Tumor volume. (B) Gross appearance of xenografts and excised tumors at day 15. Scale bar, 5mm. (C) Tumor weight at day 15. A representative result from three independent experiments with similar results is shown. Five separate experiments were performed. Error bars represent 1 SD. *indicates significance compared with control, $P < 0.05$. ** indicates significance compared with control, $P < 0.01$. (D) Effect of 2-OX in combination

with 5-FU on *Vegf* mRNA expression *in vivo*. Cells in PBS were implanted into the right flank region of seven-week-old C57BL/6J mice. Intraperitoneal injections of the indicated cocktails occurred daily beginning at day 7 after implantation. LLC tumors were removed from mice fifteen days after implantation for quantitative RT-PCR. Eight separate experiments were performed. Error bars represent 1 SD. *indicates significance compared with control, $P < 0.01$. *Vegf* mRNA levels in LLC tumors were quantified by quantitative RT-PCR and normalized to the level of *Actin* mRNA.

Acknowledgements

K. M. is a recipient of a Japan Society for the Promotion of Science Research Fellowship for Young Scientists. We thank Ms. H. Tanaka for her expert technical assistance. This work was supported in part by a Grant-in-Aid for Scientific Research on Priority Areas (17013016)(S. T.).

References

1. Folkman, J. 1971. Tumor angiogenesis: therapeutic implications. *N. Engl. J. Med.* 285: 1182-1186.
2. Gasparini, G., Longo, R., Toi, M., and Ferrara, N. 2005. Angiogenic inhibitors: a new therapeutic strategy in oncology. *Nat. Clin. Pract. Oncol.* 2: 562-577.
3. Leung DW, Cachianes G, Kuang WJ, Goeddel DV, Ferrara N. 1989. Vascular endothelial growth factor is a secreted angiogenic mitogen. *Science* 246:1306–1309.
4. Levy AP, Tamargo R, Brem H, Nathans D. 1989. An endothelial cell growth factor from the mouse neuroblastoma cell line NB41. *Growth Factors* 2:9–19.
5. Senger D, Van de Water L, Brown LF, Nagy JA, Yeo KT, Yeo TK, Berse B, Jackman RW, Dvorak AM, Dvorak HF. 1993. Vascular permeability factor (VPF, VEGF) in tumor biology. *Cancer Metastasis Rev* 12:303–324
6. Goldberg MA, Schneider T. 1994. Similarities between the oxygen-sensing mechanism regulating the expression of vascular endothelial growth factor and erythropoietin. *J Biol Chem* 269:4355–4359.
7. Plate KH, Breier G, Weich HA, Risau W. 1992. Vascular endothelial growth factor is a potential tumor angiogenesis factor in human gliomas in vivo. *Nature* 359:845–848.
8. Aiello LP, Avery RL, Arrigg PG, Keyt BA, Jampel HD, Shah ST, Pasquale LR, Thieme H, Iwamoto MA, Park JE, Nguyen HV, Aiello LM, Ferrara N, King GL. 1994. Vascular endothelial growth factor in ocular fluid of patients with diabetic retinopathy and other retinal disorders. *N Engl J Med* 331:1480–1487.
9. Sharma HS, Wunsch M, Brand T, Verdouw PD, Schaper W. 1992 a. Molecular biology

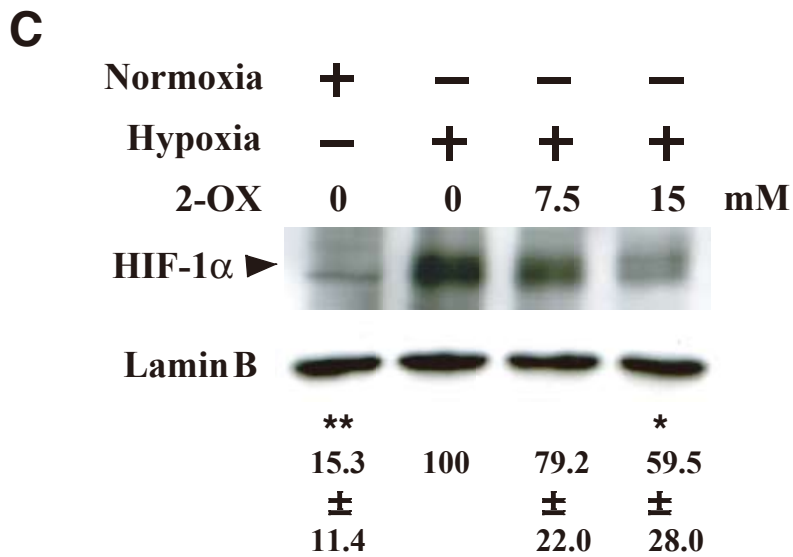
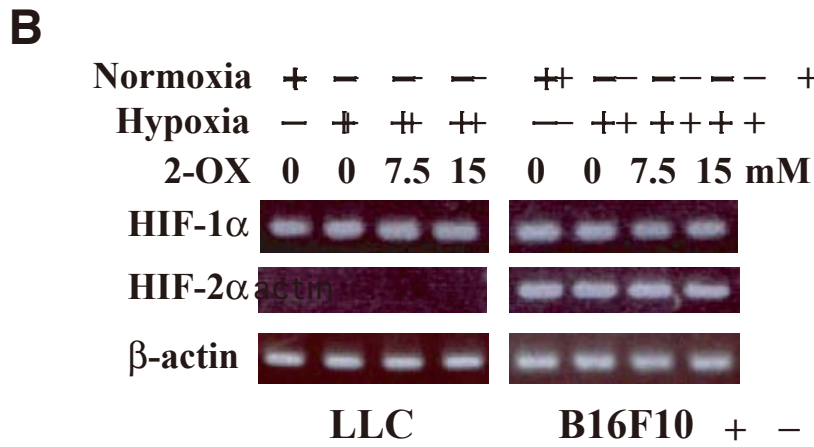
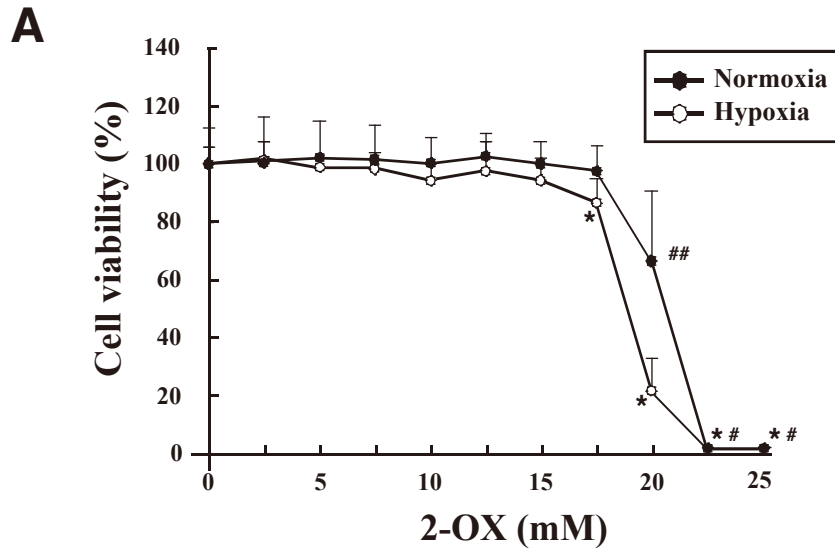
- of the coronary vascular and myocardial responses to ischemia. *J Cardiovasc Pharmacol* 20:S23–S31.
10. Sharma HS, Wunsch M, Schmidt M, Schott RJ, Kandolf R, Schaper W. 1992 b. Expression of angiogenic growth factors in the collateralize swine myocardium. *EXS (Exper Suppl)* 61:255–260.
 11. Shweiki D, Itin A, Soffer D, Keshet E. 1992. Vascular endothelial growth factor induced by hypoxia may mediate hypoxia-initiated angiogenesis. *Nature* 359:843–845.
 12. Schuster SJ, Badiavas EV, Costa-Giomi P, Weinmann R, Erslev AJ, Caro J. 1989. Stimulation of erythropoietin gene transcription during hypoxia and cobalt exposure. *Blood* 73:13–16.
 13. Goldberg MA, Gaut CC, Bunn HF. 1991. Erythropoietin mRNA levels are governed by both the rate of gene transcription and posttranscriptional events. *Blood* 77:271–277.
 14. Rondon IJ, MacMillan LA, Beckman BS, Goldberg MA, Schneider T, Bunn HF, Malter JS. 1991. Hypoxia up-regulates the activity of a novel erythropoietin mRNA binding protein. *J Biol Chem* 266:16594–16598.
 15. Semenza GL, Wang GL. 1992. A nuclear factor induced by hypoxia via de novo protein synthesis binds to the human erythropoietin gene enhancer at a site required for transcriptional activation. *Mol Cell Biol* 12:5447–5454.
 16. Wang GL, Semenza GL. 1993. Characterization of hypoxia-inducible factor 1 and regulation of DNA binding activity by hypoxia. *J Biol Chem* 268:21513–21518.
 17. Semenza GL. 2000. HIF-1 and human disease: one highly involved factor. *Genes Dev* 14:1983–1991.
 18. Iyer NV, Kotch LE, Agani F, Leung SW, Laughner E, Wenger RH, Gassmann M, Gearhart

- JD, Lawler AM, Yu AY, Semenza GL. 1998. Cellular and developmental control of O₂ homeostasis by hypoxia-inducible factor 1 α . *Genes Dev* 12:149–162.
19. Wang GL, Jiang B-H, Rue EA, Semenza GL. 1995. Hypoxia-inducible factor 1 is a basic-helix-loop-helix-PAS heterodimer regulated by cellular O₂ tension. *Proc Natl Acad Sci USA* 92:5510–5514.
 20. Maxwell PH, Wiesener MS, Chang GW, Maxwell PH, Wiesener MS, Chang GW, Clifford SC, Vaux EC, Cockman ME, Wykoff CC, Pugh CW, Maher ER, Ratcliffe PJ. 1999. The tumor suppressor protein VHL targets hypoxia-inducible factors for oxygen-dependent proteolysis. *Nature* 399:271–275.
 21. Jaakkola P, Mole DR, Tian YM, Wilson MI, Gielbert J, Gaskell SJ, Kriegsheim Av, Hebestreit HF, Mukherji M, Schofield CJ, Maxwell PH, Pugh CW, Ratcliffe PJ. 2001. Targeting of HIF- α to the von Hippel–Lindau ubiquitylation complex by O₂-regulated prolyl hydroxylation. *Science* 292:468–472.
 22. Matsumoto K, Imagawa S, Obara N, Suzuki N, Takahashi S, Nagasawa T, and Yamamoto M. 2006. 2-Oxoglutarate downregulates expression of vascular endothelial growth factor and erythropoietin through decreasing hypoxia-inducible factor-1 α and inhibits angiogenesis. *J. Cell. Physiol* 209: 333-340.
 23. Shimamura M, Nagasawa H, Aahino H, Yamamoto Y, Hazato T, Uto Y, et al. 2003. A novel hypoxia-dependent 2-nitroimidazole KIN-841 inhibits tumor-specific angiogenesis by blocking production of angiogenic factors. *Br J Cancer* 88:307–13.
 24. Ferrara N, Hillan KJ, Novotny W. Bevacizumab (Avastin), a humanized anti-VEGF monoclonal antibody for cancer therapy. *Biochem Biophys Res Commun.* 2005 Jul 29;333(2):328-35.

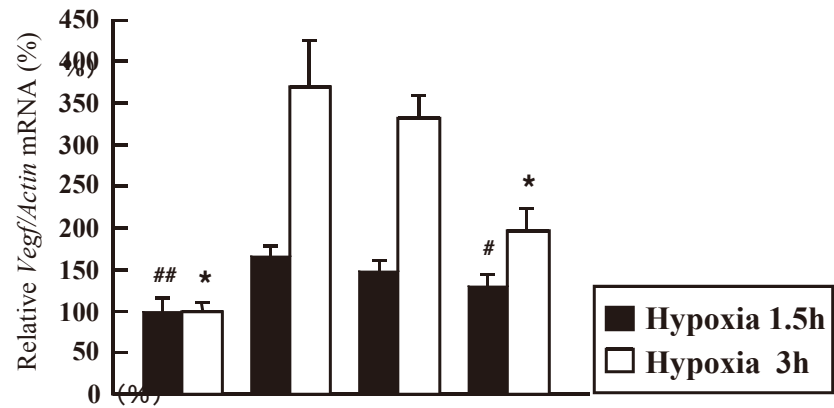
25. Huwitz H, Fehrenbacher L, Novotny W, Cartwright T, Hainsworth J, Heim W, et al. 2004. Bevacizumab plus irinotecan, fluorouracil, and leucovorin for metastatic colorectal cancer. *N Engl J Med* 350:2335–42.
26. Cunliffe CJ, Franklin TJ, Hales NJ, Hill GB. 1992. Novel inhibitors of prolyl 4-hydroxylase. 3. Inhibition by the substrate analogue N-oxalalglycine and its derivatives. *J Med Chem* 35: 2652–8.
27. Mailloux RJ, Puiseux-Dao S, Appanna VD. 2008. α -Ketoglutarate abrogates the nuclear localization of HIF-1 α in aluminum-exposed hepatocytes. *Biochimie*: Epub ahead of print.
28. MacKebzie ED, Selak MA, Tennant DA, Payne LJ, Crosby S, Frederiksen CM et al. 2007. Cell-permeating α -ketoglutarate derivatives alleviate pseudohypoxia in succinate dehydrogenase-deficient cells. *Mol Cell Biol* 27: 3282–89.
29. Choi HJ, Song BJ, Gong YD, Gwak WJ and Soh Y. 2008. Rapid degradation of hypoxia-inducible factor-1 α by KRH102053, a new activator of prolyl hydroxylase 2. *British Journal of Pharmacology*. 154. 114–125
30. Urquilla P, Fong A, Oksanen S, et al. 2004. Upregulation of endogenous erythropoietin (Epo) in healthy subjects by inhibition of hypoxia-inducible factor (HIF) prolyl hydroxylase. *Blood*. 103: Abstract #174.
31. Sabri MN, DiSciascio G, Gowley MJ, Alpert D, Vetovec GW. 1991. Coronary collateral recruitment: functional significance and relation to rate of vessel closure. *Am Heart J* 121:876–880.
32. Aiello LP, Avery RL, Arrigg PG, Keyt BA, Jampel HD, Shah ST, Pasquale LR, Thieme H, Iwamoto MA, Park JE, Nguyen HV, Aiello LM, Ferrara N, King GL.

1994. Vascular endothelial growth factor in ocular fluid of patients with diabetic retinopathy and other retinal disorders. *N Engl J Med* 331:1480–1487.

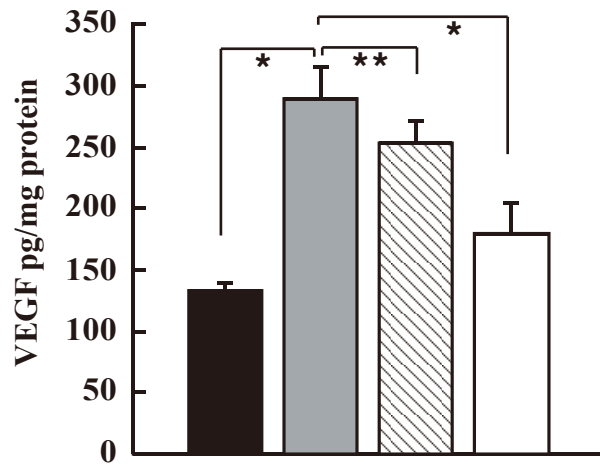
33. Arjamaa O and Nikinmaa M. 2006. Oxygen-dependent diseases in the retina: Role of hypoxia-inducible factors. *Experimental Eye Research* 83 : 473-83



Matsumoto et al., Fig.1

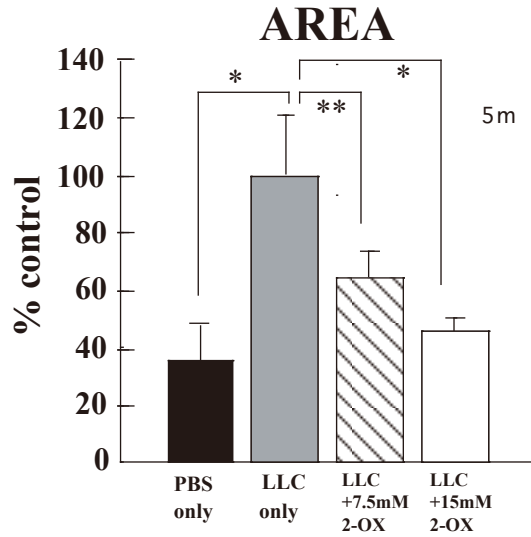
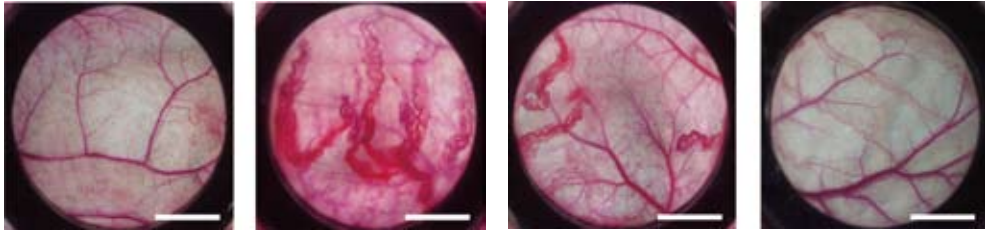
A

| | | | | |
|----------|---|---|-----|-------|
| Normoxia | + | - | - | - |
| Hypoxia | - | + | + | + |
| 2-OX | 0 | 0 | 7.5 | 15 mM |

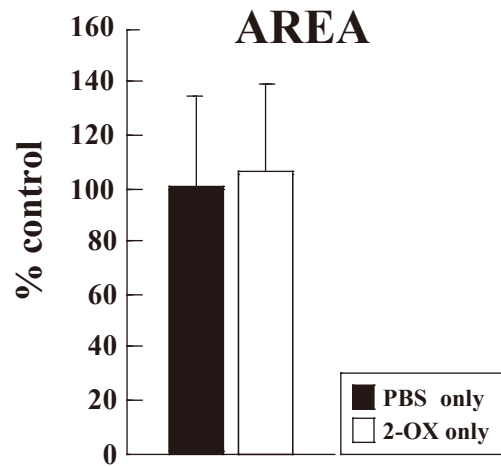
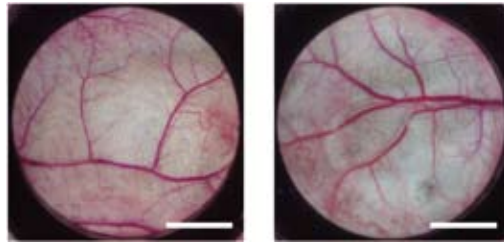
B

| | | | | |
|----------|---|---|-----|-------|
| Normoxia | + | - | - | - |
| Hypoxia | - | + | + | + |
| 2-OX | 0 | 0 | 7.5 | 15 mM |

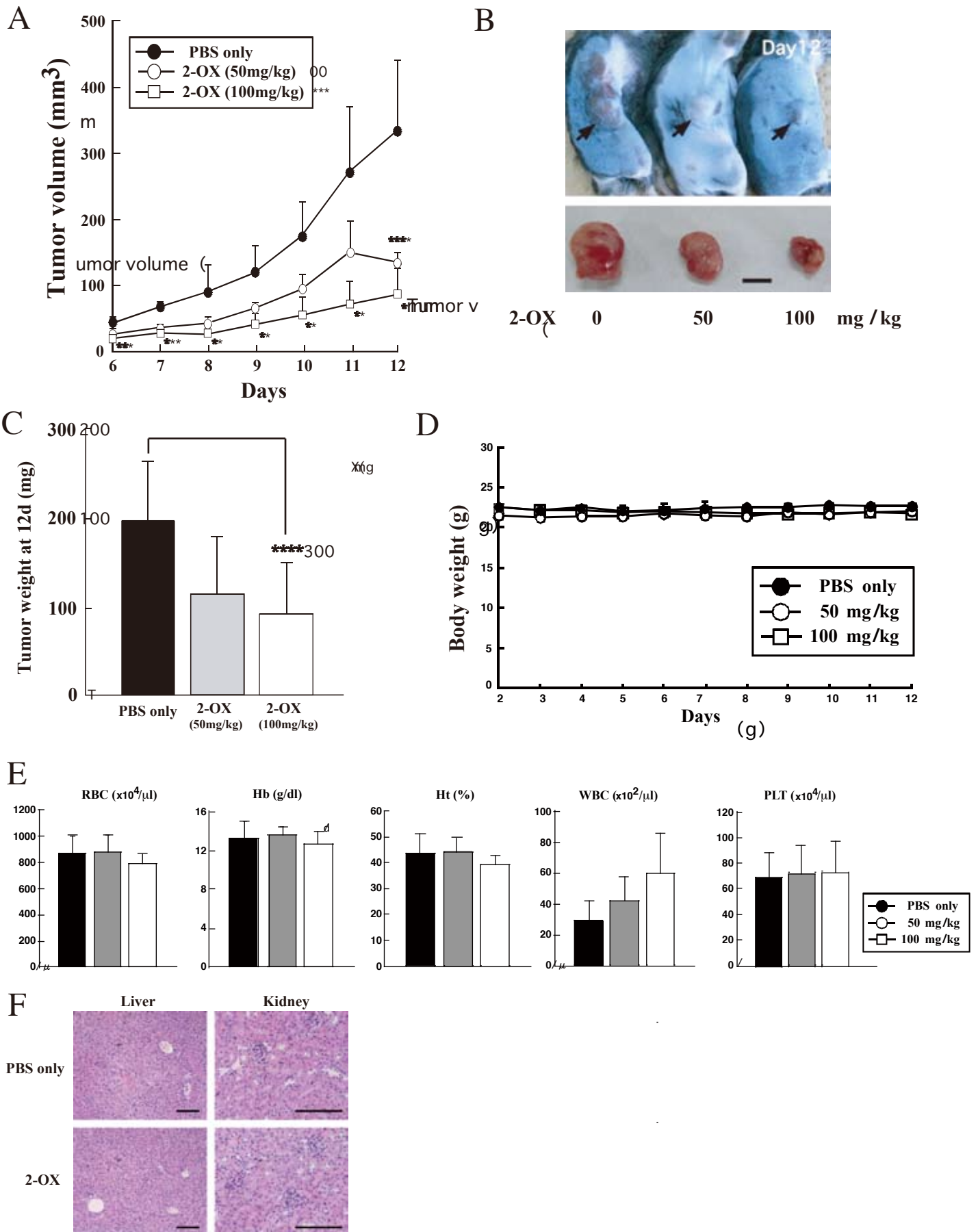
A LLC - + + +
 2-OX 0 0 7.5 15 mM



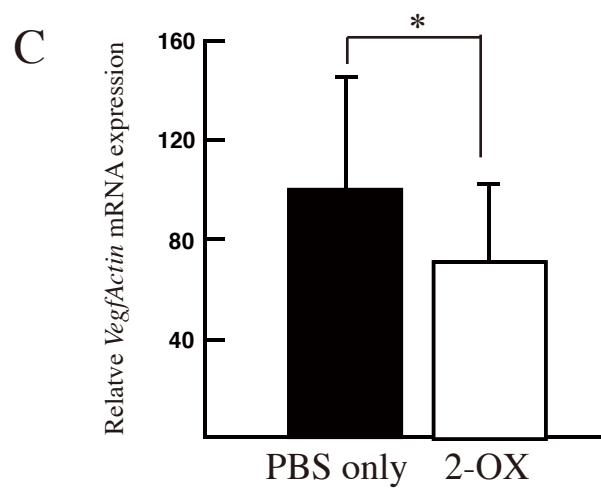
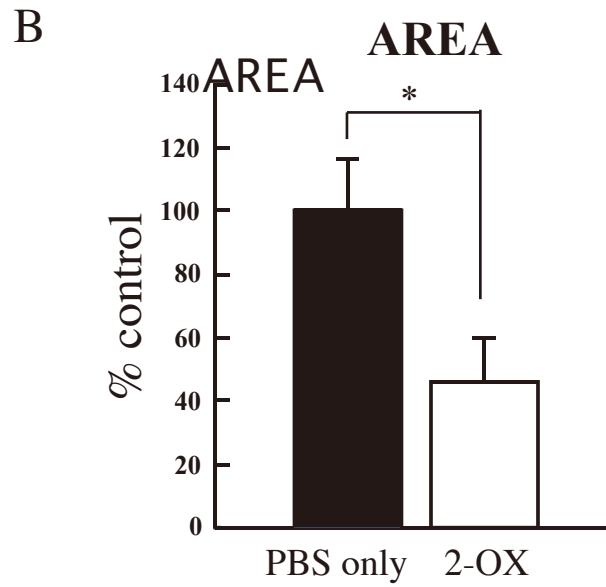
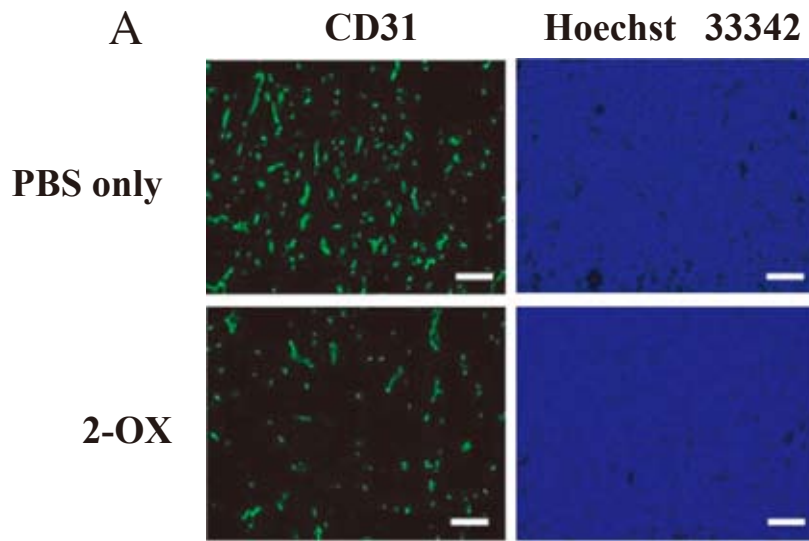
B LLC - -
 2-OX 0 15 mM

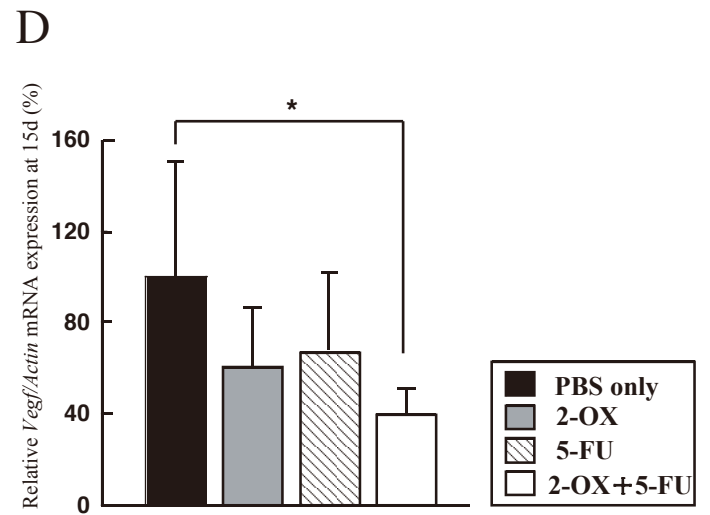
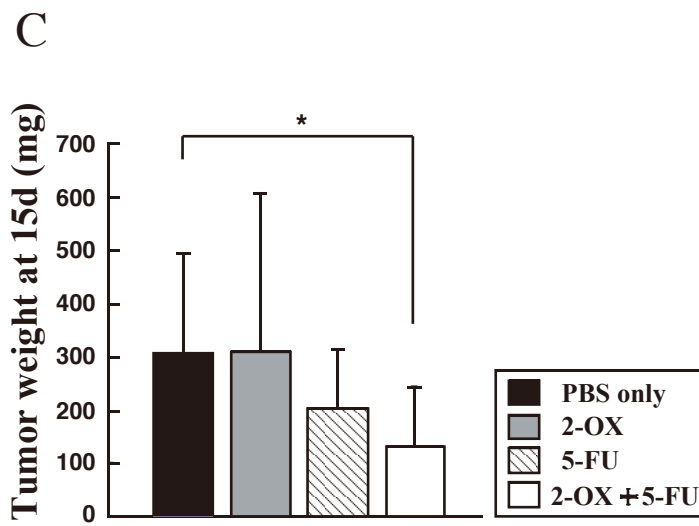
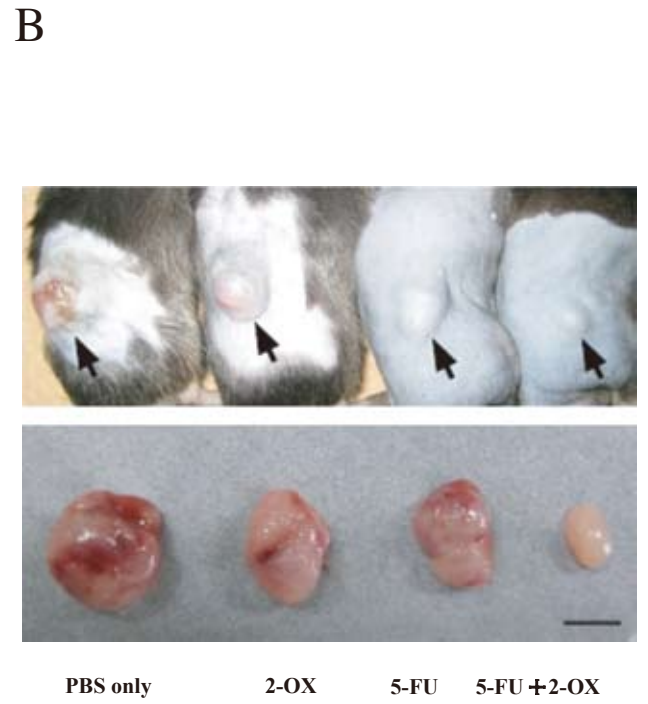
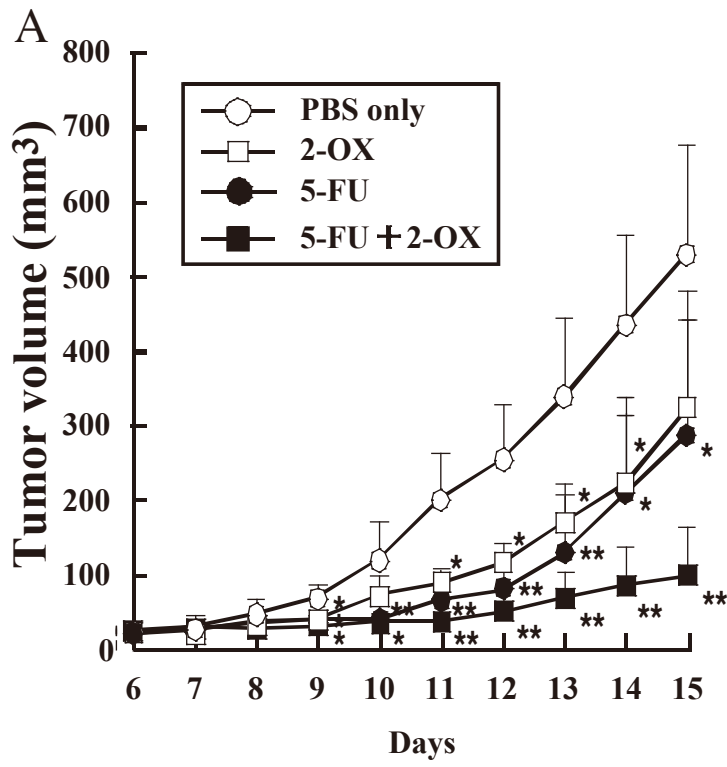


Matsumoto et al., Fig.3



Matsumoto et al., Fig.4





Matsumoto et al., Fig.6

